

Study of ion partitioning in nanoporous materials by analytical approach and molecular modeling

Jalal Dweik^a, Mahmoud Koabaz^b

Jinan University, Tripoli, Lebanon

^aJalal.douwayk@jinan.edu.lb, ^bmahmoud.koabaz@jinan.edu.lb

Corresponding author: Jalal Dweik, Jalal.douwayk@jinan.edu.lb

ABSTRACT Physical and chemical processes that occur in nano-confined aqueous solutions, particularly the role of “solute-interface” and “solute-solute” interactions within nanopores, are the source of filtration selectivity and require further investigation. The goal is to clarify the validity of different approximations based on the macroscopic mean field approach by comparing them with computational techniques such as Monte Carlo (GCMC) and classical molecular dynamics (MD). These techniques are used to study the distribution of ions at the water/nanopore interface. At the molecular scale, the results show that the distribution of ions depends on their size, polarizability and the structure of water when it is explicitly added to the model, which cannot be reproduced by the primitive model using the GCMC and the mean field approach based on the Poisson–Boltzmann equation.

KEYWORDS nanoporous materials, molecular dynamics, ions distribution, water structure

FOR CITATION Dweik J., Koabaz M. Study of ion partitioning in nanoporous materials by analytical approach and molecular modeling. *Nanosystems: Phys. Chem. Math.*, 2023, **14** (2), 172–177.

1. Introduction

Nanoporous materials have become critical components in various fields including, nanotechnology, geology, chemistry and biology [1–6]. Conventional applications of nanoporous materials include: gas and liquid separation, catalysis, energy storage, sensing, biomedical applications and environmental remediation. Understanding of ion transport provides a design guide for synthetic nanoporous membranes used in applications such as nano-filtration. The physical mechanism of ion partitioning has been studied through various approaches described below.

1.1. Donnan approach

The concept of this theory [7, 8] assumes, firstly, that the ion activities inside and outside the pore are equal to their concentrations and, secondly, the electroneutrality inside and outside the pore. The model also takes into account the presence of charged groups on the internal walls, which results in an excess of counter-ions in close proximity of the surface and a partial exclusion of co-ions in this area. When the surface charge is weak or absent, the concentration of solutes inside the pore is identical to the concentration of the bulk, and the distribution of ions becomes uniform.

1.2. Mean field approach

The theory of Poisson–Boltzmann (PB) equation explains the electrostatic interactions occurring within the pore by regarding the solvent as a continual medium and the ions in the solution as point charges. However, this leads to a lack of specificity in ion identification. The Donnan method is consistent with the mean field approach based on the PB equation for surfaces that have weak or no charge [9].

1.3. Grand canonical Monte Carlo (GCMC) simulation technique

A study by Vlachy and coworkers [10] examined the concentration profiles using a grand canonical Monte Carlo (GCMC) simulation technique. The GCMC approach, which used the primitive model [11], explicitly describes ions but treats the solvent as a continuous medium. The study investigated the exclusion of solutes from uncharged cylindrical pores using three approaches: Donnan, PBE, and GCMC using the primitive model. The concentration profiles for a pore radius of 1 nm showed that the anion was excluded near the pore surface using the GCMC approach, while both the Donnan and PB models showed a homogeneous distribution of solutes. However, due to thermal fluctuations and strong ion-ion correlations, the mean field and Donnan approaches were unable to accurately describe the exclusion of electrolytes from uncharged pores.

1.4. Classical molecular dynamics

The current understanding of ionic transport across nanopores based on macroscopic (Donnan) and mesoscopic (Primitive model using GCMC and PB) fluid physics is only partial. This paper presents a molecular simulation study [12–17] of the ions behavior at the water/nanopore interface, focusing on the effect of a neutral atomic surface from hydrophobic to hydrophilic case. The behavior of ions at the interface is characterized by determining the density distribution and the coefficient of partition.

2. Methods

2.1. Numerical method and analytical approach

We first study the ion transport for a single salt in a cylindrical nanochannel at the macroscopic mean field level, by using both a numerical method and an analytical approach. We employ a space-charge (SC) model [18] based on the nonlinear Poisson–Boltzmann (PB) equation for the electrostatic potential $\tilde{\psi}(\tilde{r})$, as well as the extended Nernst–Planck ion flux and the Stokes equations, all as a function of two dimensionless parameters: the ratio of the pore radius r_p , to the Debye length based on the feed concentration, r_p/λ_c , and the ratio of the pore radius to the Debye length based on the membrane charge density, r_p/λ_m . The Poisson–Boltzmann equation which determines the electric potential inside the pore has the following form:

$$\frac{2}{\tilde{r}} \frac{\partial}{\partial \tilde{r}} \left(r \frac{\partial \tilde{\psi}}{\partial \tilde{r}} \right) \approx \left(\frac{r_p}{\lambda_c} \right)^2 \left(e^{+\tilde{\psi}} - e^{-\tau \tilde{\psi}} \right), \quad (1)$$

where

$$\tilde{\psi} = -\frac{z_1 F \psi(x, \tilde{r})}{RT} \geq 0, \quad \tilde{r} = \frac{r}{r_p}, \quad \tau = \frac{|z_2|}{|z_1|}. \quad (2)$$

Here F is the Faraday constant, z_i is the ion valence, and λ_c is the Debye length associated with the concentration C given by:

$$\lambda_c = \left(\frac{RT\varepsilon}{2\nu_1 z_1^2 F^2 C} \right)^{1/2} \propto C^{-1/2}. \quad (3)$$

The boundary conditions at the surface and the condition at the center and of the pore can be presented in dimensionless form:

$$\left. \frac{\partial \tilde{\psi}}{\partial \tilde{r}} \right|_{\tilde{r}=1} = 4\sigma^*, \quad \left. \frac{\partial \tilde{\psi}}{\partial \tilde{r}} \right|_{\tilde{r}=0} = 0, \quad (4)$$

where

$$\sigma^* = \frac{1}{4} \left(\frac{r_p}{\lambda_m} \right)^2, \quad (5)$$

λ_m is the Debye length associated with the membrane charge density:

$$\lambda_m = \left(\frac{2\varepsilon RT}{|z_1| F^2 |X_m|} \right)^{1/2} \propto |X_m|^{-1/2}, \quad (6)$$

where X_m is defined as follows

$$X_m = \frac{2\sigma_w}{F r_p}. \quad (7)$$

The “radial equilibrium” approximation which gives one the concentration $c_i(r)$ (the Boltzmann distribution):

$$c_i(r, x) \approx k_i(x, r) \nu_i C(x), \quad (8)$$

where

$$k_i(x, r) = \exp \left[-\frac{z_i F \psi(x, r)}{RT} \right], \quad (9)$$

with $C(x)$ being the electrolyte concentration equivalent to the concentration of a bulk solution in equilibrium with the pore at position x and ν_i (the stoichiometric coefficient) represents the number of ions coming from the dissociated electrolytes. Here we take the case where there are two ionic species $I = 1$ and 2. So, the condition of electroneutrality is described by $\nu_1 z_1 + \nu_2 z_2 = 0$ or $\nu_1 |z_1| = \nu_2 |z_2|$:

$$(\text{Counter} - \text{ion})_{z_1}^{\nu_1} (\text{Co} - \text{ion})_{z_2}^{\nu_2} \longrightarrow \nu_1 (\text{Counter} - \text{ion})^{z_1} + \nu_2 (\text{Co} - \text{ion})^{z_2}.$$

The index ($i = 1$) represents the counter ions and the index ($i = 2$) represents the co-ions.

2.2. Classical molecular dynamic (MD)

In order to study the validity of both the mean field (macroscopic) theory and mesoscopic Primitive Model (implicit water, explicit ions), we performed classical Molecular Dynamics (MD) simulations that are especially suitable for investigating phenomena occurring at the nanoscale. We used the *Amber9* MD package [19] to perform NVT simulations of water (Pol3) at 300 K containing NaI at 1 M in a $30 \times 30 \times 190 \text{ \AA}^3$ simulation box (in the x -, y -, z -directions, respectively) with periodic boundary conditions in all three directions (Fig. 1). The Verlet leap frog algorithm was used to integrate the equations of motion with a time step of 1 fs. The simulations were performed at a constant temperature of 300 K using the weak coupling method thermostat [20] with a relaxation time step of 3 ps for the thermostat. Each simulation consisted of an equilibration stage of 5 ns followed by a data collection stage of 2 ns and the OH bond vibrations were frozen using the Shake algorithm [21]. The polarisable ions are described as charged soft sphere using the parameters in Table 1. The model walls consisted of neutral Lennard–Jones spheres starting at $z = 70 \text{ \AA}$ and $z = 120 \text{ \AA}$ (Table 2). The particle distribution in the nanopores and the ionic partition coefficients have been calculated from the simulation results, with $K_{PB} = C_P/C_B$, where C_P and C_B are respectively the average concentration of ions inside the pore and within the water layer (reservoirs).

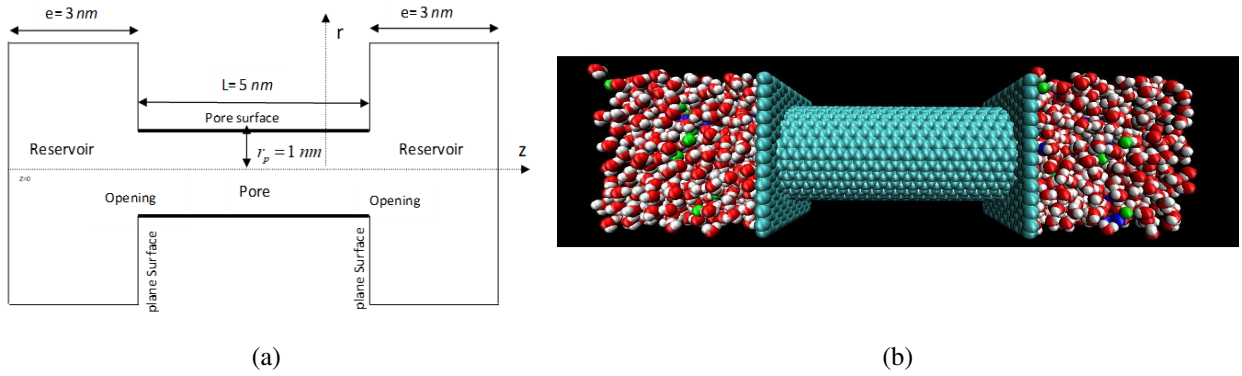


FIG. 1. The left side of the figure shows a schematic representation of the model system (a), while the right side shows a visual representation of 1 M NaI in POL3 water simulated system (b)

TABLE 1. Potential parameters for polarizable ions and polarizable rigid water POL3

| Element | σ (\AA) | ε (kcal/mol) | Charge | α_i (\AA^3) |
|---------|---------------------------|--------------------------|--------|-------------------------------|
| H | 0.000 | 0.000 | +0.365 | 0.17 |
| O | 3.210 | 0.156 | -0.730 | 0.52 |
| Na | 2.341 | 0.1 | +1 | 0.24 |
| I | 5.160 | 0.1 | -1 | 6.90 |

TABLE 2. Potential parameters for surface atoms (SA), describe the characteristics of the surface atoms

| Element | Surface nature | σ (\AA) | (kcal/mol) | Charge |
|---------|----------------|---------------------------|------------|--------|
| SA1 | hydrophobic | 2.343 | 0.03 | 0 |
| SA2 | hydrophilic | 2.343 | 1.86 | 0 |

3. Results

3.1. Analytical approach

Figure 2 shows that the behavior of the *salt-nanopore* system depends critically on the location in the r_p/λ_m vs. r_p/λ_c plane: Zones (1) and (2) demarcate the validity of the (weak potential) Debye–Huckel (DH) approximation; zones (1), (2), (3), and (5) demarcate the validity of the Extended Homogeneous (EH) approximation for which the radial variations of the potential and ionic concentrations are weak [for $r_p/\lambda_m < 2$ the *Donnan* (homogeneous) theory is

valid]; zones (5) and (6) demarcate the validity of the Good Co-ion Exclusion (GCE) approximation [22, 23] for which the salt exclusion is high because the concentration of co-ions is negligible; Zone (4) is an intermediate zone. For sufficiently high values of membrane charge, or r_p/λ_m , and/or sufficiently low values of external salt concentration, r_p/λ_c , the mean field approach breaks down due to thermal fluctuations and strong *ion-ion* correlations. The mean field approach thus becomes inaccurate in parts of zones (4) and (6), as has already been shown using the grand canonical Monte Carlo simulation technique [24] applied to the Primitive Model: for fixed external salt concentration (bulk) and small values of X_m , the simulated value for the exclusion parameter $\Gamma = 1 - \langle c_{\text{co-ion}} \rangle / c_{\text{co-ion}}$ is coherent with mean-field non-linear PB approach ($\langle c_{\text{co-ion}} \rangle / c_{\text{co-ion}}$ is the ratio of the average co-ion concentration in the pore to that in the external salt). Finally, the concentration of ions inside the nanopore approaches to the concentration in the bulk (outside the nanopore) when the surface charge of the nanopore become negligible. In this case the PB calculation and GCMC results is coherent with the experimental data [4].

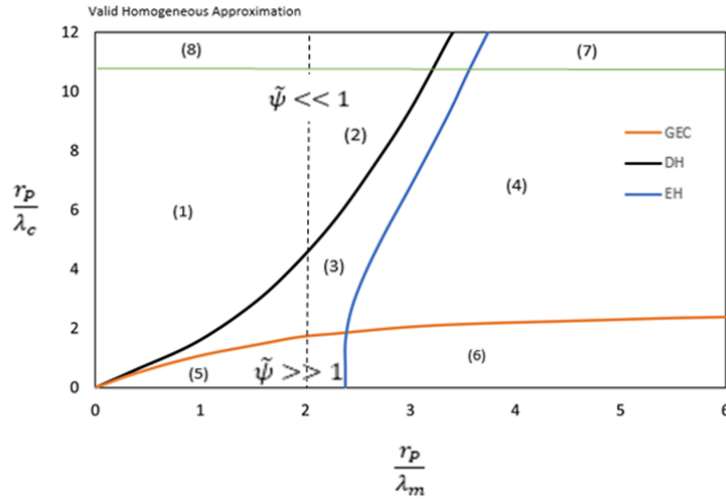


FIG. 2. Schematic Representation of the validity domain of the analytical approximations. Representation of different zones: (1) and (2): Validity of the Homogeneous and Debye–Huckel (DH), zone: (1), (2) and (3): Validity of EH zone of order 1, (5) and (6): Validity of the Homogeneous zone and inhomogeneous GEC (4): Intermediate zone (7): Validity of the plane approximation (8): Validity of the plane Debye–Huckel approximation. The blue curve delimits the area of EH. The dotted line delimits the H area

3.2. Molecular modeling

Based on molecular dynamics computing, we determine the radial distribution of water molecules and ions within the pore. Fig. 3 shows the concentration profile of ions (Na^+ and I^-) and Oxygen from water molecules (O) along the radial direction r of the nanopore in the two cases: hydrophobic and hydrophilic nanopore surface. The nature of the pore surface can influence the structure of water molecules within a pores. In hydrophilic pores, the water molecules are attracted to the nanopore surface, and, as a result, water molecules tend to form structured layers close to the nanopore surface, while it is less structured in hydrophobic pore. To further characterize the dynamics of water molecules, their self-diffusion coefficients were calculated from the derivative of the mean square displacement (MSD) along z -axis with respect to time:

$$D = \frac{1}{2t} \langle (z(t) - z(0))^2 \rangle. \quad (10)$$

The results show that the diffusion coefficient in hydrophobic nanopore surface ($1.3 \times 10^{-5} \text{ cm}^2/\text{s}$) is four times larger than the coefficient observed for the hydrophilic pore ($0.32 \times 10^{-5} \text{ cm}^2/\text{s}$). In this situation, the classical idea of image charge, which suggests that ions are repelled from the surface, does not hold true. Instead, when considering larger ions such as iodide, the volume fraction that these ions occupy becomes significant and results in higher free energy costs. As a result, these ions tend to move towards the hydrophobic interface. The way large polarizable I^- anions are distributed at the water/hydrophobic nanopore interface is similar to how they are distributed at the water/vapor interface [25], where they are found at the interface. Fig. 3(a) shows that the I^- anion peak is located below the water molecule peak at $r = 6 \text{ \AA}$, while in Fig. 3(b), it is at $r = 3 \text{ \AA}$, indicating that there is a higher concentration of I^- anions towards the hydrophilic center of the pore. In this zone, the number of the water molecules is low, whereas the Na^+ cations are located at the center of the pore, where they are hydrated by water molecules as a result of their small size and low polarizability. As mentioned above, the size effect is a critical factor that impacts how ions are adsorbed and distributed at the interface between water and nanopores. The reason for this size effect is due to the energy required to solvate ions, as their presence

can interfere with hydrogen bonding. On one hand, small solutes (such as Na^+) can be easily solvated by water molecules without disrupting the hydrogen bonding network, which means that there is no exclusion of these ions. On the other hand, large solutes (such as I^-) cannot be solvated without significantly hindering the process. The partition coefficient of I^- anions to measure the effect of the pore's surface properties (hydrophobic/hydrophilic) on the concentration of these ions inside the pore is calculated. The partition coefficient for the hydrophilic surface ($K_{PB} = 0.60$) is larger than for the hydrophobic surface ($K_{PB} = 0.52$). This result is consistent with the radial distribution obtained inside the pore (Fig. 3), which shows more I^- anions inside the pore for the hydrophilic surface compared to the hydrophobic surface.

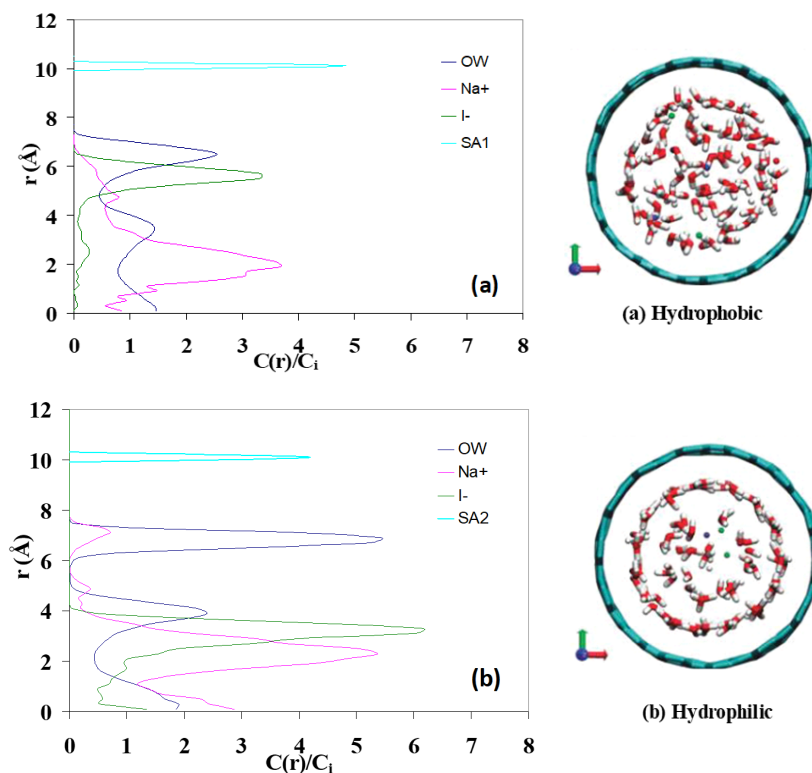


FIG. 3. The left side shows the ratio of concentration profile, $C(r)/C_i$, (C_i – concentration in the bulk phase) for polarizable sodium/iodide (NaI) ions and water molecules (a) hydrophobic pore and (b) hydrophilic pore in radial direction. The right side of Fig. 3 shows a snapshot in the direction opposite to the z -axis in the interval ($50 \text{ \AA} < z < 70 \text{ \AA}$). The color convention used is: oxygen (O) in red; hydrogen (H) in white; sodium (Na) in blue; iodide (I) in green; and wall atom in light blue.

4. Conclusion

This paper provides a description of a MD simulation study focusing on the behavior of water and ions in nanoporous media. The primitive model and macroscopic mean field based on PB equation, which treat the solvent as a dielectric continuum, are unable to explain the results presented in the paper. The simulations highlight the importance of the atomic surface in the phase behavior of electrolyte solutions in contact with the nanopore surface. Our results indicate that due to the surface influences the distribution of water at the interface is well structured. Water structures play a significant role in the distribution of ions in the system. In this study, the behavior of NaI aqueous electrolyte's cations and anions was examined in nanopore. Different behaviors were observed among the cations and anions, as some were found within the pore center and others were adsorbed at the pore interface. In hydrophobic nanopores, small Na^+ cations tended to be in the pore center, while large polarizable I^- anions tended to accumulate at the interface. On the other hand, in hydrophilic nanopores, the anions tended to concentrate in the center of the pore. The water structure and distribution of ions in the system were affected by surface effects. The distribution of ions in the system was mainly dependent on their size and polarizability, particularly, to the large I^- anion and the small Na^+ cation. The advantages of the current simulation and interpretation technique can easily be extended to a large class of synthetic nano-materials in the presence of various ionic solutions. More extensive MD simulations are being conducted to better understand the behavior of the nanoporous system under investigation and to determine the validity domains of macro- and mesoscopic approaches.

References

- [1] Dresner L., Kraus K.A. Ion exclusion and salt filtering with porous ion-exchange materials. *J. Phys. Chem.*, 1963, **67**, P. 990–998.
- [2] Jacazio G., Probst R.F., Sonin A.A., Yung D. Electrokinetic salt rejection in hyperfiltration through porous materials: Theory and experiments. *J. Phys. Chem.*, 1972, **76**, P. 4015–4023.
- [3] Siwy Z., Fulinski A. Origin of Noise in Membrane Channel Currents. *Phys. Rev. Lett.*, 2002, **89**, P. 158101–158104.
- [4] Crozier P.S., Rowley R.L. Molecular dynamics simulation of continuous current flow through a model biological membrane channel. *Phys. Rev. Lett.*, 2001, **86**, P. 2467–2470.
- [5] Roux B., Karplus M. Molecular dynamics simulations of the gramicidin channel. *Annu. Rev. Biophys. Biomol. Struct.*, 1994, **23**, P. 731–761.
- [6] Jardat M., Hribar-Lee B., Vlachy V. Self-diffusion of ions in charged nanoporous media. *Soft Matter*, 2012, **8**, P. 954–964.
- [7] Donnan F.G. The theory of membrane equilibrium and membrane potential in the presence of a non-dialyzable electrolyte. A contribution to physical-chemical physiology. *Z. Für Elektrochem. Und Angew. Phys. Chem.*, 1911, **17**, P. 572–581.
- [8] Palmeri J., Blanc P., Larbot A., David P. Theory of pressure-driven transport of neutral solutes and ions in porous ceramic nanofiltration membranes. *J. Membrane Sci.*, 1999, **160** (2), P. 141–170.
- [9] Chang C.W., Chu C.W., Su Y.S., Yeh L.H. Space charge enhanced ion transport in heterogeneous polyelectrolyte/alumina nanochannel membranes for high-performance osmotic energy conversion. *J. Mater. Chem. A*, 2022, **10**, P. 2867–2875.
- [10] Jamnik B., Vlachy V.J. Ion Partitioning between Charged Micropores and Bulk Electrolyte Solution. Mixtures of Mono- and Divalent Counterions and Monovalent Co-Ions. *Am. Chem. Soc.*, 1995, **117** (30), P. 8010–8016.
- [11] Dubois M., Zemb T., Belloni L., Deville A., Levitz P., Setton R. Osmotic pressure and salt exclusion in electrostatically swollen lamellar phases. *J. Chem. Phys.*, 1992, **96**, P. 2278–2286.
- [12] Hartnig C., Witschel C., Spohr E., Bunsenges Ber. Molecular dynamics study of electrolyte-filled pores. *Phys. Chem.*, 1998, **102**, P. 1689–1692.
- [13] Boiteux C., Kraszewski S., Ramseyer C., Girardet C. Ion conductance vs. pore gating and selectivity in KcsA channel: modeling achievements and perspectives. *J. of Molecular Modeling*, 2007, **13**, P. 699–713.
- [14] Allen T.W., Kuyucak S., Chung S.H. Molecular dynamics study of the KcsA potassium channel. *Biophys. Chem.*, 2000, **86**, P. 1–14.
- [15] Compoin M., Carloni P., Ramseyer C., Girardet C. Molecular dynamics study of the KcsA channel at 2.0-angstrom resolution: stability and concerted motions within the pore. *Biochimica Biophysica Acta – Biomembranes*, 2004, **1661**, P. 26–39.
- [16] Corry B., Allen T.W., Kuyucak S., Chung S.H. A model of calcium channels. *Biochim. Biophys. Acta*, 2000, **1509**, P. 1–6.
- [17] Berendsen H.J.C., Postma J.P.M., Van Gunsteren W.F., Dinola A., Haak J.R. Molecular dynamics with coupling to an external bath. *J. Chem. Phys.*, 1984, **81** (8), P. 3684–3690.
- [18] Caldwell J.W., Kollman P.A. Structure and Properties of Neat Liquids Using Nonadditive Molecular Dynamics: Water, Methanol, and N-Methylacetamide. *J. Phys. Chem.*, 1995, **99** (16), P. 6208–6219.
- [19] Gupta A., Rajan A.G., Carter E.A., Stone H.A. Ionic Layering and Overcharging in Electrical Double Layers in a Poisson-Boltzmann Model. *Phys. Rev. Lett.*, 2020, **125**, 1103.
- [20] Caldwell J.W., Kollman P.A. Structure and Properties of Neat Liquids Using Nonadditive Molecular Dynamics: Water, Methanol, and N-Methylacetamide. *J. Phys. Chem.*, 1995, **99** (16), P. 6208–6219.
- [21] Hijnen H.J.M., Van Daalen J., Smit J.A.M.J. The application of the space-charge model to the permeability properties of charged microporous membranes. *Colloid Interface Sci.*, 1985, **107**, P. 525–539.
- [22] Palmeri J., Blanc P., Larbot A., David P. Theory of pressure-driven transport of neutral solutes and ions in porous ceramic nanofiltration membranes. *J. Membrane Sci.*, 1999, **160**, P. 141–170.
- [23] Case D.A., et al. *AMBER9*. University of California, San Francisco, 2006.
- [24] Jungwirth P., Tobias D.J. Specific ion effects at the air/water interface. *Chem. Rev.*, 2002, **106**, P. 1259–1281.
- [25] Chandler D. Interfaces and the driving force of hydrophobic assembly. *Review Nature*, 2005, **437**, P. 640–647.

Submitted 23 February 2023; revised 18 March 2023; accepted 24 March 2023

Information about the authors:

Jalal Dweik – Professor in Mathematics and Physics, Jinan University, Zaytoun Abi-Samra, P.O. Box: 808, Tripoli, Lebanon; ORCID 0009-004-2988-0918; Jalal.douwayk@jinan.edu.lb

Mahmoud Koabaz – Assistant Professor in Mathematics and Physics, Jinan University, Zaytoun Abi-Samra, P.O. Box: 808, Tripoli, Lebanon; ORCID 0000-0003-0370-1120; mahmoud.koabaz@jinan.edu.lb

Conflict of interest: the authors declare no conflict of interest.